High-resolution spatial and temporal microscopy with intense-laser-induced rescattering electrons

2009 J. Phys.: Conf. Ser. 194 012011

(http://iopscience.iop.org/1742-6596/194/1/012011)

Journal of Physics: Conference Series **194** (2009) 012011 doi:10.1088/1742-6596/194/1/012011

High-resolution Spatial and Temporal Microscopy with Intense-laser-induced Rescattering Electrons

Toru Morishita[1,2], Toshihito Umegaki[1], Shinichi Watanabe[1], and C. D. Lin[3]

[1]Department of Applied Physics and Chemistry, University of Electro-Communications, 1-5-1 Chofu-ga-oka, Chofu-shi, Tokyo, 182-8585, Japan
[2]PRESTO, Japan Science and Technology Agency, Kawaguchi, Saitama 332-0012, Japan
[3]Department of Physics, Kansas State University, Manhattan, Kansas 66506, USA

Abstract. Following the recent developments in intense laser techniques, ultrafast phenomena of the order of a few femtoseconds to attoseconds have been discussed. We are developing new methods for ultrafast imaging for transient atomic and molecular systems. We apply the recently developed quantitative rescattering theory together with a fitting procedure to extract effective potentials as well as elastic differential cross sections of the target ions with free electrons within the single active electron model. Using experimental photoelectron spectra for rare gas atoms of Ne, Ar, Kr, and Xe, we show that the extracted atomic potentials are in good agreement with those obtained theoretically. The current method of retrieval does not require precise knowledge of the peak laser intensities. The results show that accurate charge distribution of target ions indeed can be retrieved from experimental photoelectron spectra generated by lasers, thus paving the way for using infrared laser pulses for dynamic chemical imaging of transient states of molecules with temporal resolution of few femtoseconds.

1. Introduction

X-ray diffraction and electron diffraction are the conventional methods for imaging matters to achieve spatial resolution of better than sub-Angstroms, but they are incapable of achieving temporal resolutions of femto to tens of femtoseconds, required for following chemical and biological transformations. To image such transient events, unique facilities like ultrafast electron diffraction method [1] or large facilities such as x-ray free-electron lasers (XFELs) are being developed. Instead of pursuing these evolving technologies, here we provide the needed quantitative analysis to show that existing few-cycle infrared lasers may be implemented for ultrafast imaging of transient molecules.

When an atom is exposed to an infrared laser, the atom is first tunnel ionized with the release of an electron. This electron is placed in the oscillating electric field of the laser and may be driven back to revisit its parent ion. This reencounter incurs various elastic and inelastic electron-ion collision phenomena where the structural information of the target is embedded[2]. The possibility of using such laser-induced returning electrons for self-imaging molecules has been frequently discussed[3, 4, 5, 6, 7]. It is reported that the outermost molecular orbital of the N_2 molecule can be extracted from the high-order harmonic generation (HHG) spectra using the tomographic procedure[8]. This interesting result has generated a lot of excitement, but the reported results are based on a number of assumptions[9, 10, 11]. To make dynamic chemical

imaging with infrared lasers as a practical tool, general theoretical considerations, especially on the validity of the extraction procedure, should be given carefully.

Recently we have developed a quantitative rescattering (QRS) theory for laser induced high-energy photoelectron spectra and HHG spectra[12, 13, 14]. We demonstrated that the elastic differential cross sections (DCS) of free electrons by the target ions can be accurately extracted from the photoelectron spectra[16, 17, 18]. We also showed that the accurate photo-recombination cross sections can be extracted from HHG spectra[19]. Our conclusions are based on accurate theoretical solutions of the time dependent Schrödinger equation [20, 21] as well as experimental results by different groups[16, 17, 18]. Further, it is shown that using numerically obtained DCS for rare gas atoms with intrinsic random errors, the effective potentials between free electron and the target ions, or the charge densities of the target ions, can be accurately retrieved by a fitting procedure using a Genetic algorithm[22]. These results indicates the possibility of re-constructing the structural information of a transient molecule using laser induced photoelectron spectra and HHG spectra.

In the present work, we outline our recent progress on the ultrafast imaging, based on the QRS theory. We also present a new result of retrieving the effective potentials for rare gas atoms directly from existing experimental photoelectron spectra generated by intense laser pulses.

2. Outline of the quantitative rescattering theory

The detailed explanation of the QRS theory for photoelectron spectra [13] and HHG spectra[14] has been given previously, thus only the essential points are given here.

In the QRS theory, we establish that experimental high-energy photoelectron momentum distributions, $S(\mathbf{p})$, can be expressed simply by using the returning electron momentum $\mathbf{p}_r$,

$$S(\mathbf{p}) = W(p_r)\sigma_{exp}(p_r, \theta_r), \tag{1}$$

where $\sigma_{exp}(p_r, \theta_r)$ is the elastic DCS of free electrons with momentum p_r, by the target ion. Here θ_r is the scattering angle with respect to the direction of the returning electron along the polarization. $W(p_r)$ is interpreted as the momentum distribution of the returning electrons, to be called the returning wave packet in this work. A detailed expression of the returning wave packet has been derived analytically based on a fully quantum mechanical adiabatic theory[15]. We use the fact that the electron spectra exhibit cylindrical symmetry along the laser polarization for atomic targets. It is shown that the relation between the returning electron momentum (p_r, θ_r) and the photoelectron momentum (p, θ) in the laboratory frame can be written as

$$p_z = p\cos\theta = \pm(p_r/1.26 - p_r\cos\theta_r), \tag{2}$$

$$p_y = p\sin\theta = p_r\sin\theta_r, \tag{3}$$

where along the z- and y-axes are parallel and perpendicular to the polarization direction, respectively, and the "+" and "−" signs in Eq. (2) refer to cases where the electrons collides with the ion from the "right" and the "left", respectively, and this relation is shown in Fig. 1(a). Note that $p_r/1.26 = A_r$, where $A_r = A(t_r)$ is the vector potential at the time, $t = t_r$, when the electron returns to the core. Similarly $p_r = p_r(t_r)$ is the electron momentum at the time of the return. The relation $p_r/1.26 = A_r$ states that the returning electron momentum is determined by the vector potential at the returning time only. This relation with the coefficient of 1.26 would give the maximum collision energy of about 3 U_p, when the electrons return at the time when the vector potential is near the maximum. According to this relation, the peak laser intensity does not enter Eqs.(2) and (3), thus we are able to decouple the two terms on the right-hand side of Eq. (1). Note that the term $p_r/1.26 = A_r$ in Eq. (2) means that an additional momentum $\pm A_r$ will be added to the momentum of the photoelectron along the polarization direction as it exits the laser field. (See Fig. 1(a).)

Since $\sigma_{exp}(p_r, \theta_r)$ as well as the relation between (p_r, θ_r) and (p, θ) is independent of laser intensity, we can integrate Eq. (1) over focus volume to obtain

$$S_{I_0}(\mathbf{p}) = \bar{W}_{I_0}(p_r)\sigma_{exp}(p_r, \theta_r), \tag{4}$$

where $S_{I_0}(\mathbf{p})$ is the volume-integrated photoelectron momentum distributions from a laser beam which has a peak intensity of I_0 at the laser focus, and $\bar{W}_{I_0}(p_r)$ is the volume-integrated wave packet, namely,

$$\bar{W}_{I_0}(p_r) = \rho \int_0^{I_0} W_I(p_r) \left(-\frac{\partial V}{\partial I}\right) dI \tag{5}$$

with $W_I(p_r)$ being the wave packet for the laser pulse at a single intensity I and ρ being the density of the target gas. Here, $-(\partial V/\partial I)dI$ represents the volume element for having the intensity between I and $I + dI$. Since $S_{I_0}(\mathbf{p})$ describes the 2D electron momentum distributions measured experimentally, we can use Eq. (4) to extract the DCSs and the effective potentials.

3. Extracting elastic electron-ion scattering cross sections and charge densities from experimental high-energy photoelectron momentum spectra

Eq. (4) shows that the experimental 2D electron momentum distributions, $S_{I_0}(\mathbf{p})$, for photoelectrons can be expressed as the product of a volume-integrated wave packet, $\bar{W}_{I_0}(p_r)$, and elastic DCS, $\sigma_{exp}(p_r, \theta_r)$, of the target ion with electrons. If one can calculate $\bar{W}_{I_0}(p_r)$ or obtain it in some other ways, then the DCS can be extracted from Eq. (4). In our previous work[18, 19, 13, 14], we showed that the wave packet can be conveniently calculated and the obtained cross sections were compared with experimental results. Then, the extracted DCS can be used to find the effective potentials by a fitting procedure as in Ref. [22]. In the present work, the effective potentials are searched directly, without knowing the laser parameters, from the photoelectron distribution by the least square fitting, minimizing the sum

$$\chi^2(\Xi) = \sum_{ij} \left[\frac{\sigma(p_i, \theta_j; \Xi)}{\sigma(p_i, \theta_0; \Xi)} - \frac{\sigma_{exp}(p_i, \theta_j)}{\sigma_{exp}(p_i, \theta_0)}\right]^2, \tag{6}$$

where $\sigma(p, \theta; \Xi)$ is the DCS calculated using the effective potential described by a set of fitting parameters, Ξ, and the angle θ_0 is fixed to normalize the DCS. Since the wave packet, $\bar{W}_{I_0}(p_r)$, is independent of the scattering angle θ_r, the ratio of the experimental DCSs can be evaluated by the relation $\frac{\sigma_{exp}(p_i,\theta_j)}{\sigma_{exp}(p_i,\theta_0)} = \frac{S(\mathbf{p})|_{(p_r=p_i,\theta_r=\theta_j)}}{S(\mathbf{p})|_{(p_r=p_i,\theta_r=\theta_0)}}$ using Eq. (4). On the other hand, the theoretical DCS, $\sigma(p, \theta; \Xi)$, is obtained from the solution to the time-independent Schrödinger equation in the single active electron approximation using the effective potential used in ref. [23, 24], which is parametrized in the form

$$V(r; \Xi = \{Z, \xi, \eta\}) = -Z_{eff}(r)/r, \tag{7}$$

where the effective charge $Z_{eff}(r)$ reads

$$Z_{eff}(r) = (Z-1)\left[1 - \left\{(\eta/\xi)(e^{\xi r} - 1) + 1\right\}^{-1}\right] - Z. \tag{8}$$

Note that the effective charge $Z_{eff}(r)$ goes to 1 for large r, and to the nuclear charge of the target atom, Z, at $r = 0$. It is also empirically found that $\xi \sim 1$ and $\eta \sim Z^{0.4}$ for all elements[24]. Thus we search the fitting parameters in the ranges of $Z = [1, 100]$, $\xi = [0.5, 6.5]$, and $\eta = [Z^{0.4} - 1, Z^{0.4} + 1]$ to find the minimum of $\chi^2(\Xi)$ n Eq. (6). To find the parameters

for each target efficiently, we use the Genetic Algorithm[25] used in Ref. [22] as well as Powell's method[26]. We note that the shape of the model potentials as well as the calculated DCSs are almost the same as those used in ref. [22].

We apply the QRS theory together with the fitting procedure described above to analyze the experimental photoelectron spectra of rare gas atoms generated by 800 nm, 100 fs, $\sim 10^{14}$ W/cm^2 intense laser pulses, which are reported in refs. [16, 18]. In Fig. 1(a), we show the 2D experimental photoelectron spectrum of Ne at the laser intensity of $I_0 = 3.5 \times 10^{14}$ W/cm^2 (The precise intensity of the experiment is not important). In Fig. 1(b), we replot the high-energy part of the spectra between the two dashed circles in Fig. 1(a) as a function of the rescattering electron momentum, (p_r, θ_r). To smooth out the above threshold ionization (ATI) peaks, the electron spectra in Fig. 1(b) are obtained by integrating over a bin of $\Delta p_r = 0.05$ a.u. and $\Delta\theta_r = 10°$. In Fig. 1(c), we show the effective charge, $Z_{eff}(r)$, extracted from the experimental data by the fitting procedure, normalizing the DCSs at $\theta_0 = 170°$. Note that the calculated DCSs for fitting are also convoluted using the same size of the bin as the experimental one. In Fig. 1(d) we also show the experimental DCS obtained from the relation $\frac{\sigma_{exp}(p_i,\theta_j)}{\sigma_{exp}(p_i,\theta_0)}\sigma(p_i,\theta_0;\Xi)$ with the best fit.

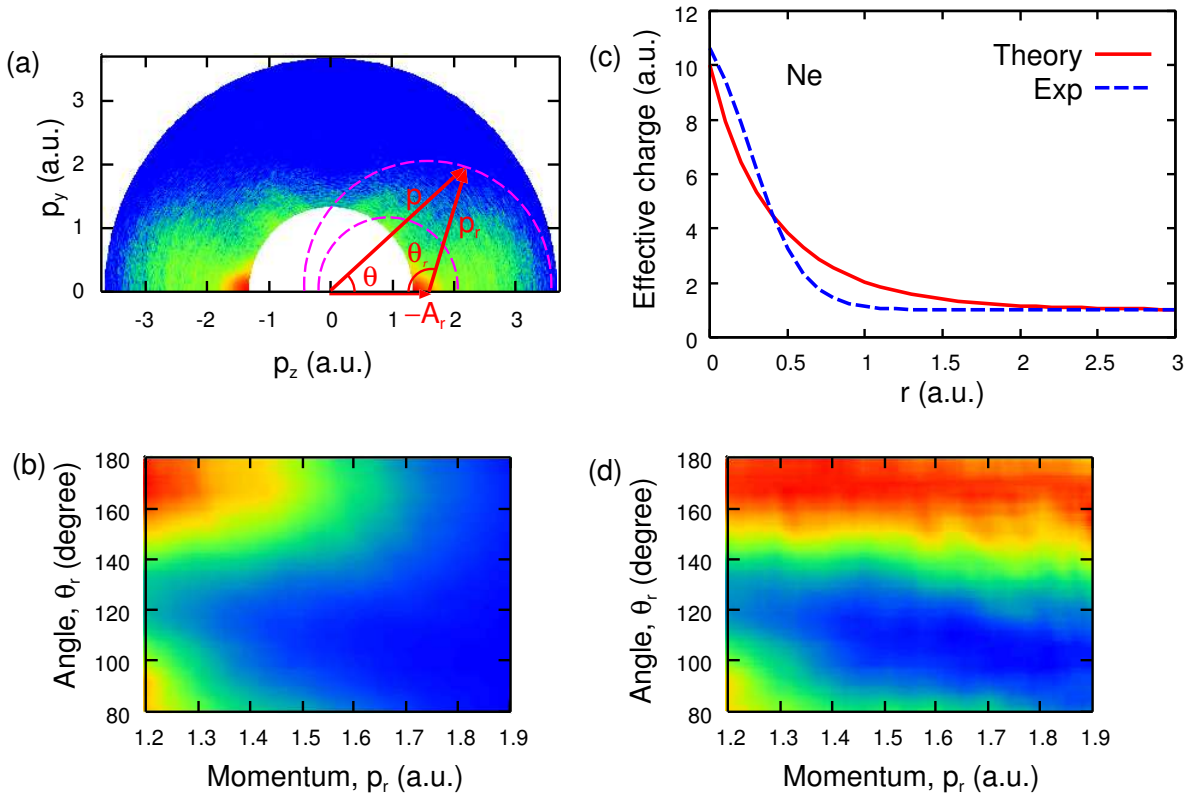

Figure 1. (a) Two-dimensional photoelectron distribution of Ne in a 100 fs laser pulse at the peak intensity of 3.5×10^{14} W/cm^2. The image is plotted in logarithmic scale. (b) High-energy part of the photoelectron distributions between the dotted circles in Fig. 1(a) for large angles as a function of the rescattering electron momentum, (p_r, θ_r) in linear scale. (c) Effective charge extracted from experimental data using a fitting procedure. (d) Elastic differential cross sections extracted from experimental data using a fitting procedure.

We applied the same method to extract the effective charge and the DCS from the experimental data for Ar, Kr, and Xe. The extracted DCS are shown in the left column of Fig. 2

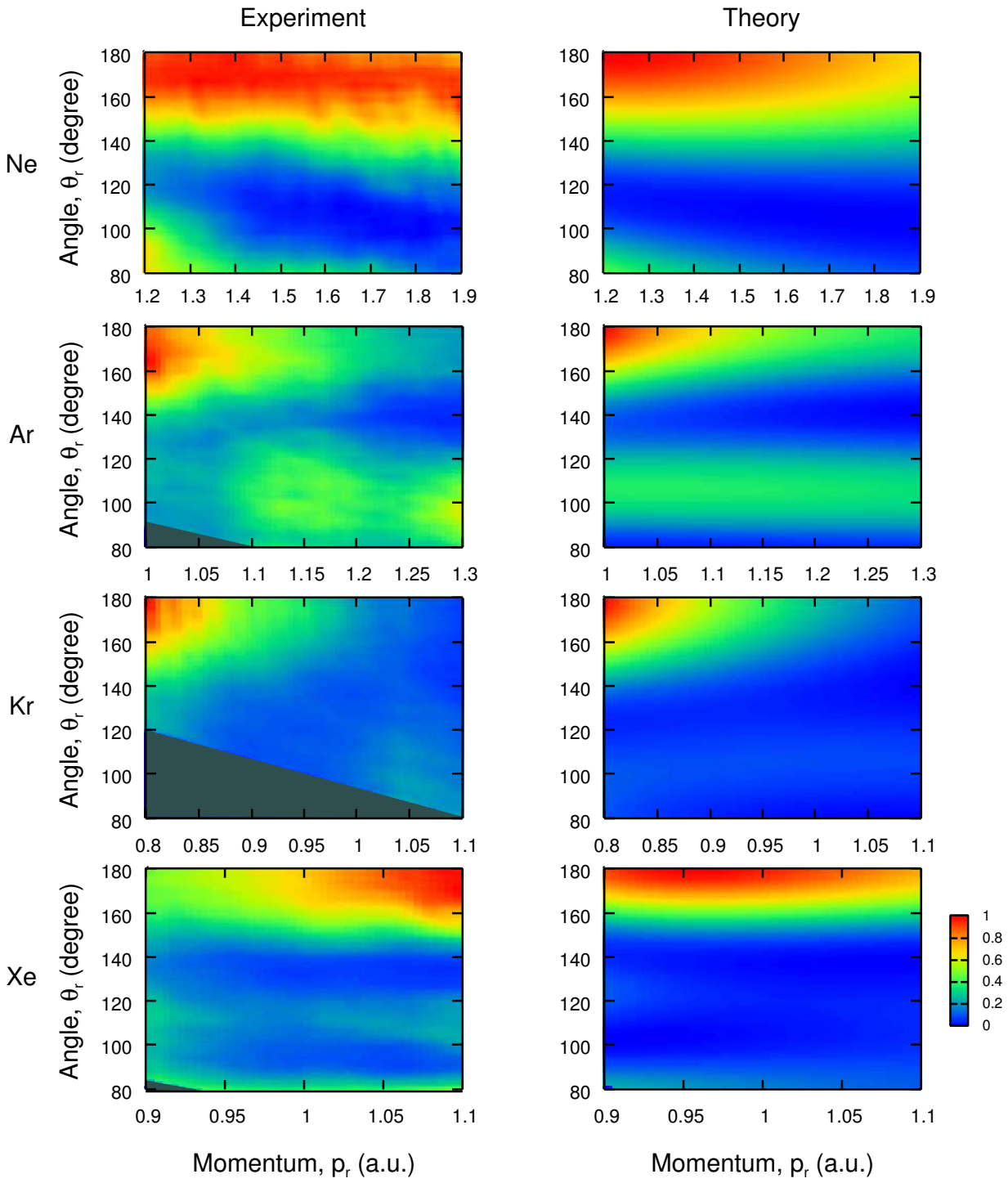

Figure 2. Elastic differential cross sections extracted from experimental data (left) and calculated in the single active electron approximation (right). The dark triangles in the lower left corners on the left column indicate the regions where no photoelectron data are available.

together with the one from Ne. On the right-hand column, the DCS calculated theoretically in the single active electron approximation using the effective potentials with the parameters

tabulated in ref. [24] are shown. We can see a large degree of agreement between each pair of the DCSs in a broad range of angles and energies.

We also compare the reconstructed effective charges from experimental data with those from the model potential in [24]. We can see good agreements between them. Indeed, the nuclear charges of Z =10.6, 15.1, 38.8, and 50.1 for Ne, Ar, Kr, and Xe obtained from the fitting procedure are close to those for the real atoms within 20%.

Looking into more details, the discrepancy between the effective potentials extracted from experimental data and from theory is larger for Ne, although the agreement between the cross sections is fairly good. We looked at the shape of $\chi^2(\Xi)$ around the minimum for Ne graphically, and found that the minimum is very shallow in (Z, η, ξ) space. Indeed, the DCSs calculated using the two effective potentials in Fig. 3 for Ne almost coincide with each other, indicating that wider region of photoelectron momentum distributions are needed to determine more accurate potential.

This result indicates that the QRS model in the form of Eq. (4) together with the fitting procedure in Eq. (6) works very well, and one can use laser-induced high-energy photoelectron spectra to probe the target atom structure.

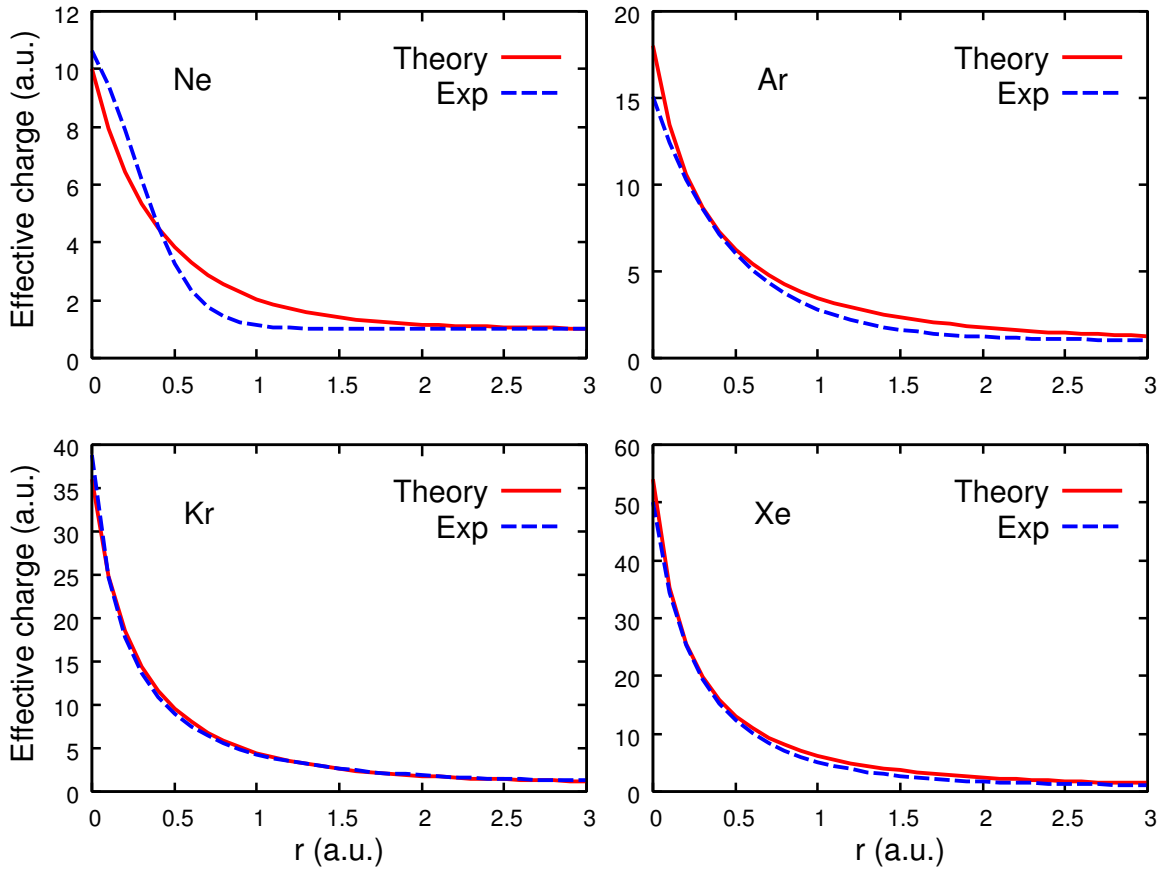

Figure 3. Comparison of theoretical and experimental effective charges extracted from photoelectron momentum spectra.

4. Summary and Outlook

In this work we have successfully extracted the elastic scattering differential cross sections (DCS) as well as the effective potential between the singly charged ions of rare gas atoms and free

electrons from the momentum distributions of high-energy photoelectrons generated by infrared laser pulses. The essential idea is based on the recently developed quantitative rescattering (QRS) theory [12, 13, 14] together with the fitting procedure[22]. In the QRS theory, we have shown that high-energy photoelectron momentum distributions can be expressed as the product of a returning electron wave packet with the DCS for the collision between free electrons and target ions at large angles. In particular, the theory has been shown to apply to experimental electron spectra where photoelectrons are collected from spatially distributed laser intensities. It is possible to apply the present method to extract effective charge and DCS for more complex molecular targets. High-energy photoelectron momentum distributions has become available for isotropically distributed[27] and partially aligned[28] molecules. Since probe pulses with duration of a few femtoseconds are readily available these days, this method can be used for dynamic chemical imaging with temporal resolution of a few femtoseconds. Our results presented in this work show that the effect of collecting electrons from the whole laser focus volume and the lack of precise knowledge of lasers do not limit this versatile method by using appropriate fitting procedure. The present results thus serve to illustrate that dynamic chemical imaging of atomic and molecular targets with infrared lasers indeed is possible [29].

Acknowledgment

We would like to thank A. T. Le, Z. Chen, K. Ueda, and M. Okunishi for stimulating discussions. This work was supported in part by the PRESTO program of JST, Japan, by Grants-in-Aid for Scientific Research from JSPS, Japan, and in part by the Chemical Sciences, Geosciences and Biosciences Division, Office of Basic Energy Sciences, Office of Science, U.S. Department of Energy.

References

[1] A. Zewail, Annu. Rev. Phys. Chem. **57**, 65 (2006).
[2] P. B. Corkum, Phys. Rev. Lett.**71**, 1994 (1993).
[3] T. Zuo, A. D. Bandrauk and P. B. Corkum, Chem. Phys. Lett. **259**, 313 (1996).
[4] M. Spanner, O. Smirnova, P. B. Corkum and M. Y. Ivanov, J. Phys. B: At. Mol. Opt. Phys. **37**, L243 (2004).
[5] S. X. Hu, L. A. Collins, Phys. Rev. Lett. **94**, 073004 (2005).
[6] M. Lein, J. P. Marangos, and P. L. Knight, Phys. Rev. A **66**, 051404(R) (2002).
[7] S. N. Yurchenko, S. Patchkovskii, I. V. Litvinyuk, P. B. Corkum, and G. L. Yudin, Phys. Rev. Lett. **93**, 223003 (2004).
[8] J. Itatani J. Levesque, D. Zeidler, H. Niikura, H. Pépin, J. C. Kieffer, P. B. Corkum, and D. M. Villeneuve, Nature **432**, 867 (2004).
[9] V. H. Le A.-T. Le, R.-H. Xie, and C. D. Lin, Phys. Rev. A. (2007).
[10] S. Patchkovskii, Z. Zhao, T. Brabec, and D. M. Villeneuve, Phys. Rev. Lett. **97**, 123003 (2006).
[11] J. Levesque, D. Zeidler, J. P. Marangos, P. B. Corkum, and D. M. Villeneuve, Phys. Rev. Lett. **98**, 183903 (2007).
[12] T. Morishita, A.-T. Le, Z. Chen, and C. D. Lin, Phys. Rev. Lett. **100**, 013903 (2008).
[13] Z. Chen, A-T. Le, T. Morishita, and C. D. Lin, Phys. Rev. A 79, 033409 (2009).
[14] A. T. Le, R. R. Lucchese, S. Tonzani, T. Morishita, and C. D. Lin Phys. Rev. A **80**, 013401 (2009).
[15] O. I. Toltikhin, T. Morishita, and S. Watanabe, submitted (2009).
[16] M. Okunishi, T. Morishita, G. Prümper, K. Shimada, C. D. Lin, S. Watanabe, and K. Ueda, Phys. Rev. Lett. **100**, 143001 (2008).
[17] D. Ray, B. Ulrich, I. Bocharove, C. Maharjan, P. Ranitovic, B. Gramkow, B. Gramkow, M. Magrakvelidze, S. De, I. V. Litvinyuk, A. T. Le, T. Morishita, C. D. Lin, G. G. Paulus, and C. L. Cocke, Phys. Rev. Lett. **100**, 143002 (2008).
[18] T. Morishita, M. Okunishi, K. Shimada, G. Prümper, K. Shimada, Z. Chen, S. Watanabe, K. Ueda, and C. D. Lin, J. Phys. B: At. Mol. Opt. Phys. **42**, 105205 (2009)
[19] S. Minemoto, T. Umegaki, Y. Oguchi, T. Morishita, A.-T. Le, S. Watanabe, and H. Sakai, Phys. Rev. A **78**, 061402 (2008).
[20] Z. Chen, T. Morishita, A.-T. Le, M. Wickenhauser, X. M. Tong, and C. D. Lin Phys. Rev. A 74, 053405 (2006).

[21] T. Morishita, Z. Chen, S. Watanabe, and C. D. Lin, Phys. Rev. A **75**, 023407 (2007).
[22] J. Xu, H.- L. Zhou, Z. Chen, and C. D. Lin, Phys. Rev. A **79**, 052508 (2009).
[23] A. E. S. Green, D. L. Sellin, and A. S. Zachor, Phys. Rev. **184**, 1 (1969).
[24] R. H. Garvey, C. H. Jackman, and A. E. S. Green, Phys. Rev. A **12**, 1144 (1975).
[25] D. L. Carroll, FORTRAN genetic algorithm driver, 1999, http://cuaerospace.com/carroll/ga.html in Developments in Theoretical and Applied Mechanics XVIII, edited by H. Wilson, R. Batra, C. Bert, A. Davis, R. Schapery, D. Stewart, and F. Swinson (School of Engineering, The University of Alabama, Tuscaloosa, 1996), pp. 411-424.
[26] W. H. Press, S. A. Teukolsky, W. T. Vetterling, B. P. Flannery, Numerical Recipes: The Art of Scientific Computing (FORTRAN Version) (Cambridge University Press, New York, NY, 1992).
[27] M. Okunishi, R. Itaya, K. Shimada, G. Prümper, K. Ueda, M. Busuladžić, A. Gazibegović-Busuladžić, B. Milošević, and W. Becker, J. Phys. B **41**, 201004 (2008).
[28] M. Meckel, D. Comtois, D. Zeidler, A. Staudte, D. Pavičić, H. C. Bandulet, H. Pépin, J. C. Kieffer, R. Dörner, D. M. Villeneuve, and P. B. Corkum, Science **320**, 1478 (2008).
[29] T. Morishita, A.-T. Le, Z. Chen, and C. D. Lin, New J. Phys. **10**, 025011 (2008).